J Physiol Sci (2011) 61:515–523
DOI 10.1007/s12576-011-0173-8

ORIGINAL PAPER

Sarcomere length-dependent Ca^{2+} activation in skinned rabbit psoas muscle fibers: coordinated regulation of thin filament cooperative activation and passive force

Norio Fukuda · Takahiro Inoue · Mitsunori Yamane · Takako Terui · Fuyu Kobirumaki · Iwao Ohtsuki · Shin'ichi Ishiwata · Satoshi Kurihara

Received: 19 July 2011 / Accepted: 10 August 2011 / Published online: 7 September 2011

Abstract In skeletal muscle, active force production varies as a function of sarcomere length (SL). It has been considered that this SL dependence results simply from a change in the overlap length between the thick and thin filaments. The purpose of this study was to provide a systematic understanding of the SL-dependent increase in Ca^{2+} sensitivity in skeletal muscle, by investigating how thin filament "on–off" switching and passive force are involved in the regulation. Rabbit psoas muscles were skinned, and active force measurements were taken at various Ca^{2+} concentrations with single fibers, in the short (2.0 and 2.4 μm) and long (2.4 and 2.8 μm) SL ranges. Despite the same magnitude of SL elongation, the SL-dependent increase in Ca^{2+} sensitivity was more pronounced in the long SL range. MgADP (3 mM) increased the rate of rise of active force and attenuated SL-dependent Ca^{2+} activation in both SL ranges. Conversely, inorganic phosphate (Pi, 20 mM) decreased the rate of rise of active force and enhanced SL-dependent Ca^{2+} activation in both SL ranges. Our analyses revealed that, in the absence and presence of MgADP or Pi, the magnitude of SL-dependent Ca^{2+} activation was (1) inversely correlated with the rate of rise of active force, and (2) in proportion to passive force. These findings suggest that the SL dependence of active force in skeletal muscle is regulated via thin filament "on–off" switching and titin (connectin)-based interfilament lattice spacing modulation in a coordinated fashion, in addition to the regulation via the filament overlap.

Keywords Muscle mechanics · Ca^{2+} sensitivity · Troponin · Titin

Abbreviations

SL	Sarcomere length
PLV	Porcine left ventricular muscle
cTn	Porcine left ventricular troponin
sTn	Rabbit fast skeletal troponin

Introduction

Striated muscle, either skeletal or cardiac, exhibits sarcomere length (SL) dependence of active force generation. It is well established that this SL dependence involves a mechanism by which Ca^{2+} sensitivity of active force increases upon SL elongation in skeletal and cardiac muscles (e.g., [1, 2]). It is generally thought that skeletal muscle can operate over a broad SL range (i.e., ~1.6 to ~3.6 μm) and indeed displays both ascending and descending limbs of the SL-active force curve, in contrast to cardiac muscle that normally exhibits only the ascending limb (e.g., [2, 3]).

A well-known study by Gordon et al. [3] demonstrated that the SL dependence of active force generation in skeletal muscle is a simple, linear function of the overlap length between the thick and thin filaments. However, the findings of later studies have suggested that a change in the thick–thin filament overlap is not the sole factor underlying the SL dependence, and additional mechanisms are

Electronic supplementary material The online version of this article (doi:10.1007/s12576-011-0173-8) contains supplementary material, which is available to authorized users.

N. Fukuda (✉) · T. Inoue · T. Terui · F. Kobirumaki · I. Ohtsuki · S. Kurihara
Department of Cell Physiology,
The Jikei University School of Medicine, Tokyo, Japan
e-mail: noriof@jikei.ac.jp

M. Yamane · S. Ishiwata
Department of Physics, Waseda University, Tokyo, Japan

likewise involved. Allen and Moss [4] reported that a reduction in interfilament lattice spacing plays a pivotal role in SL-dependent Ca^{2+} activation in the short SL range (~1.6 to ~2.5 μm; i.e., on the ascending limb). More recently, Shimamoto et al. [5] extended this finding by using single myofibrils of rabbit psoas muscle and confirmed that a change in the lattice spacing of only ~1.0 nm causes a dramatic change in active force over a broad range of SL (~2.2 to ~3.8 μm), under conditions where active force is elicited not only by Ca^{2+} but also by MgADP (and subsequent formation of strongly bound, actomyosin–ADP cross-bridges via thin filament cooperative activation).

Unlike in cardiac muscle where SL-dependent Ca^{2+} activation forms the basis for the Frank–Starling law of the heart (e.g., [6] and references therein), the physiological significance of the length dependence in skeletal muscle is still not fully understood. Recently, however, Llewellyn et al. [7] reported that SL dramatically varies in skeletal muscle (gastrocnemius muscle in mice) in vivo upon electric stimulation, in the relatively long SL range of ~2.6 to ~3.0 μm. Given the significance of this previous work, we consider that it is of importance to systematically investigate how active force production varies in response to SL elongation in both the short and long SL ranges, at various thin filament activation levels, because the operating SL range may vary depending on various factors, such as the type of muscle or the animal species.

In the present study, by using skinned single fibers of rabbit psoas muscle, we investigated SL-dependent Ca^{2+} activation in two different SL ranges (short range, 2.0–2.4 μm, and long range, 2.4–2.8 μm) under conditions where thin filament cooperative activation is varied by the application of MgADP or Pi [8].

Materials and methods

All experiments performed in this study conformed to the Guide for the Care and Use of Laboratory Animals (1996, National Academy of Sciences, Washington, DC, USA). Also, all experiments were performed in accordance with the Guidelines on Animal Experimentation of The Jikei University School of Medicine (Tokyo, Japan).

Preparation of skinned muscle and muscle mechanics

Muscle strips (1–2 mm in diameter and ~10 mm in length) were dissected from psoas muscle of white rabbits (2–3 kg) in Ca^{2+}-free Tyrode's solution containing 30 mM 2,3-butanedione monoxime (BDM) (as in [8–11]). Rabbit psoas muscles were skinned in relaxing solution [5 mM MgATP, 40 mM BES, 1 mM Mg^{2+}, 10 mM EGTA, 1 mM dithiothreitol, 15 mM phosphocreatine, 15 U/ml creatine phosphokinase, 180 mM ionic strength (adjusted by K-propionate), pH 7.0] containing 1% (w/v) Triton X-100 and 10 mM BDM overnight at ~3°C. Muscles were stored for up to 3 weeks at −20°C in relaxing solution containing 50% (v/v) glycerol. All solutions contained protease inhibitors [0.5 mM phenylmethylsulfonyl fluoride (PMSF), 0.04 mM leupeptin, 0.01 mM E64].

Isometric active and passive forces were measured at 15°C, according to the method in our previous studies with single fibers at SL 2.0 and 2.4 μm (or at SL 2.4 and 2.8 μm) [9–11]. Briefly, the single fiber was first immersed in relaxing solution, and SL was set at 2.0 μm. SL was measured by laser diffraction during relaxation. Active and passive forces were measured at SL 2.0 μm, and 20 min after elongation of SL to 2.4 μm (at which time passive force reached the quasi-plateau level), force measurements were repeated, as described in our previous studies [8, 10]: rundown <10% for active and passive forces in all cases. In some experiments, active and passive forces were measured at SL 2.4 and then at 2.8 μm (rundown <10% for active and passive forces in all cases). MgADP or inorganic phosphate (Pi) was added to the individual activating solutions in accordance with our previous studies [8, 12, 13]. When active force was measured, pCa was adjusted by Ca/EGTA [8–14].

Because titin-based passive force reportedly increases from ~0 mN/mm^2 at SL ~2.0 μm in an exponential manner in rabbit psoas muscle [10, 15], we used SL 2.0 μm as the control SL in the present study. Also, considering our previous finding that maximal Ca^{2+}-activated force was greatest at SL ~2.4 μm in rabbit psoas muscle under the same experimental condition [9], we investigated the effects of MgADP or Pi on SL-dependent Ca^{2+} activation at SL 2.0–2.4 μm (i.e., on the ascending limb) and 2.4–2.8 μm (i.e., on the descending limb). The difference between the values of the mid-point of the force–pCa curve (i.e., pCa_{50}) at SL 2.0 (or 2.4) and 2.4 (or 2.8) μm was used as an index of the SL dependence of Ca^{2+} sensitivity (expressed as ΔpCa_{50}; [8, 10, 12–14]). The steepness of the force–pCa curve was expressed as n_H. At the end of the active and passive force measurement, single fibers were treated with KCl/KI (e.g., [14, 15]), and the ratio of titin-based passive force to total passive force was obtained. Because titin-based (KCl/KI-sensitive) passive force was ~100% at SL 2.4 and 2.8 μm in all cases (as in [15]), we disregarded the contribution of non-titin-based passive force in the present analysis.

For the measurement of the rate of rise of active force, SL was set at 2.0 μm in relaxing solution. Then, the preparation was immersed in low-EGTA (0.5 mM) relaxing solution for 1 min, and transferred to the control activating solution (pCa 4.5) without MgADP or Pi, followed

by relaxation. Then, the procedure was repeated in the presence of MgADP or Pi, and the time to half-maximal activation was compared with that obtained in the preceding contraction in the same preparation, hence minimizing the effect of diffusion that is dependent upon the muscle thickness (see [8]). The ratio of the time to half-maximal activation, defined as $t_{1/2}$, was used as an index of cooperative activation [8].

Troponin treatment

Troponin (Tn) treatment was performed based on our previously published procedure (see [8, 10, 11, 16] and references therein). Briefly, after performing the force–pCa protocol without any treatment, the skinned fiber was bathed in rigor solution (10 mM BES, 150 mM K-propionate, 2.5 mM EGTA, 5 mM $MgCl_2$, pH 7.0), containing the whole cardiac troponin complex (cTn, 6 mg/ml; extracted from bovine left ventricular muscle) or the whole skeletal troponin complex (sTn, 2 mg/ml; extracted from rabbit fast skeletal muscle), and 80 mM BDM for 60 min at 25°C. As noted in our previous report [10], the presence of BDM was essential to avoid contraction upon treatment and the ensuing damage to the sarcomere structure. Then, the preparation was washed with normal relaxing solution at 15°C for 10 min with gentle agitation to remove excess Tn molecules. The results of our previous studies demonstrated that the exchange ratio for cTn (or the Tn complex with bovine left ventricular TnT) and sTn (or the Tn complex with rabbit fast skeletal TnT) was ~50 and ~100%, respectively, in skinned rabbit psoas muscle fibers [10, 16].

Statistics

Significant differences were assigned using the paired or unpaired Student's *t* test as appropriate. Data are expressed as mean ± SEM, with *n* representing the number of muscles. Linear regression analyses were performed in accordance with the method used in previous studies [10, 17]. Statistical significance was assumed to be $P < 0.05$. NS indicates $P > 0.05$.

Results

Effect of MgADP or Pi on the rate of rise of active force

First, we investigated the effect of various concentrations of MgADP (0–10 mM) or Pi (0–20 mM) on the rate of rise of active force. We found that MgADP significantly decreased $t_{1/2}$ at low concentrations (1 and 3 mM) but increased $t_{1/2}$ at a high concentration (10 mM), and Pi exerted similar effects at low (3 and 5 mM) and high (20 mM) concentrations (Fig. 1a, b). The accelerating effect of MgADP was greatest at 3 mM, and the decelerating effect of Pi became significant at 20 mM. Therefore, in the following experiments, we used 3 mM MgADP to enhance thin filament cooperative activation and 20 mM Pi to reduce it, based on our previous study on porcine left ventricular muscle (PLV) (cf. [8]).

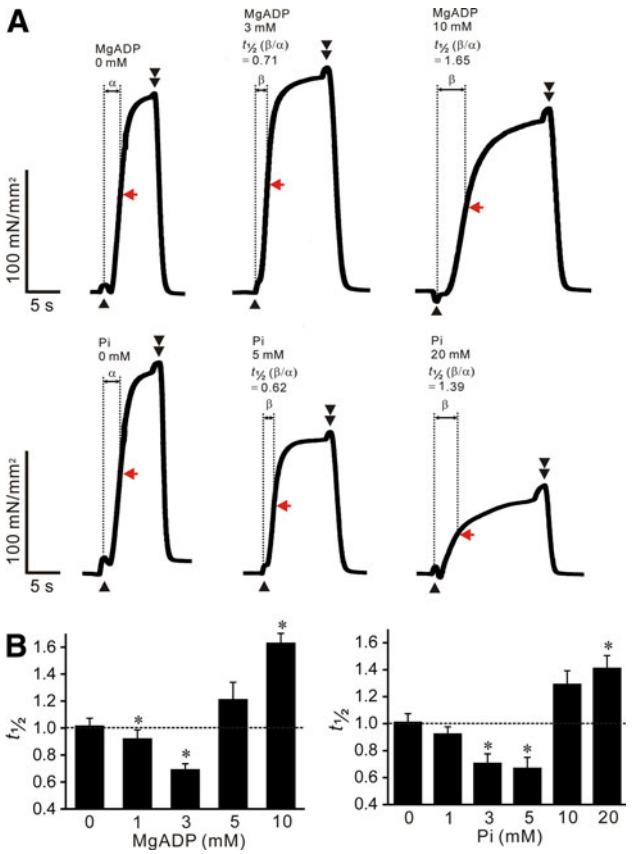

Fig. 1 Effects of MgADP or Pi on the rate of rise of active force in rabbit psoas muscle fibers; pCa 4.5, SL 2.0 μm. **a** Typical chart recordings showing active force responses in the absence and presence of MgADP (*top*) or Pi (*bottom*). Data obtained from the same preparation for either MgADP or Pi. *Black arrowheads* and *double arrowheads* indicate the points at which the solution was switched from low-EGTA (0.5 mM) relaxation to contraction and from contraction to high-EGTA (10 mM) relaxation, respectively. Because of a change in surface tension, a hump was caused upon solution switch from low-EGTA (0.5 mM) relaxation to contraction and from contraction to high-EGTA (10 mM) relaxation. The time to half-maximal activation (50%) was measured as indicated by α and β, and the relative value, i.e., β/α, was obtained for each preparation and defined as $t_{1/2}$ [8]. *Red arrow* in each record, 50% of maximal force. **b** Graph summarizing the effects of various concentrations of MgADP (*left*) or Pi (*right*) on $t_{1/2}$. $^*P < 0.05$ compared with 0 mM MgADP or Pi. Note that $t_{1/2}$ is ~1.0 in the absence of MgADP or Pi, indicating reproducibility of the rate of rise of active force (as in [8]); $n = 6$ for both MgADP and Pi

Effects of MgADP or Pi on SL-dependent Ca^{2+} activation in the short SL range

Next, we investigated the effect of MgADP or Pi on SL-dependent Ca^{2+} activation in the short SL range, i.e., 2.0–2.4 μm. Under the control condition without MgADP or Pi, an increase in SL from 2.0 to 2.4 μm increased maximal Ca^{2+}-activated force (as in [9]) and increased Ca^{2+} sensitivity of force by ~0.15 pCa units (i.e., ΔpCa_{50}; see Fig. 2a, b; Table 1).

We found that 3 mM MgADP shifted the force–pCa curve leftward to a greater magnitude at SL 2.0 μm than at 2.4 μm, and consequently decreased ΔpCa_{50} (Fig. 2a). Conversely, 20 mM Pi shifted the force–pCa curve rightward to a greater magnitude at SL 2.0 μm than at 2.4 μm, and consequently increased ΔpCa_{50} (Fig. 2b). The effects of 3 mM MgADP or 20 mM Pi on $t_{1/2}$ are summarized in Fig. 2c (the preparations used for Fig. 2a, b). The values of pCa_{50}, n_H and maximal force at SL 2.0 and 2.4 μm under various conditions are summarized in Table 1.

Consistent with the finding of our previous study [10], cTn treatment shifted the force–pCa curve rightward to a greater magnitude at SL 2.0 μm than at 2.4 μm, and consequently increased ΔpCa_{50} (Fig. 3a). However, sTn treatment did not affect Ca^{2+} sensitivity at either SL. Accordingly, ΔpCa_{50} was not significantly altered by sTn treatment. cTn treatment increased $t_{1/2}$ (as in [10]); however, sTn treatment did not significantly alter it. The values of pCa_{50}, n_H and maximal force at SL 2.0 and 2.4 μm with and without cTn or sTn treatment are summarized in Table 2.

In Fig. 4, we summarize the relationship between $t_{1/2}$, pCa_{50} and ΔpCa_{50} obtained under various conditions, i.e., in the presence of MgADP or Pi, and cTn or sTn treatment. As found in PLV [8], a significant linear relationship was obtained in each graph, with the slope for rabbit psoas muscle being lower than that for PLV in a relationship of $t_{1/2}$ versus pCa_{50} (Fig. 4b) and that of $t_{1/2}$ versus ΔpCa_{50} (Fig. 4c).

Effects of MgADP or Pi on SL-dependent Ca^{2+} activation in the long SL range

We then investigated the effect of MgADP or Pi on SL-dependent Ca^{2+} activation in the long SL range, i.e., 2.4–2.8 μm. Under the control condition without MgADP or Pi, an increase in SL from 2.4 to 2.8 μm lowered maximal Ca^{2+}-activated force (as in [9]) but it increased Ca^{2+} sensitivity of force by ~0.20 pCa units (i.e., ΔpCa_{50}; see Fig. 5a; Table 3). This magnitude of increase was significantly greater than that observed when SL was varied between 2.0 and 2.4 μm (Fig. 5a).

As observed in a study in the short SL range, MgADP at 3 mM shifted the force–pCa curve leftward, to a magnitude greater at SL 2.4 μm than at 2.8 μm, and consequently decreased ΔpCa_{50} (Fig. 5b). Conversely, Pi at 20 mM shifted the force–pCa curve rightward, to a magnitude

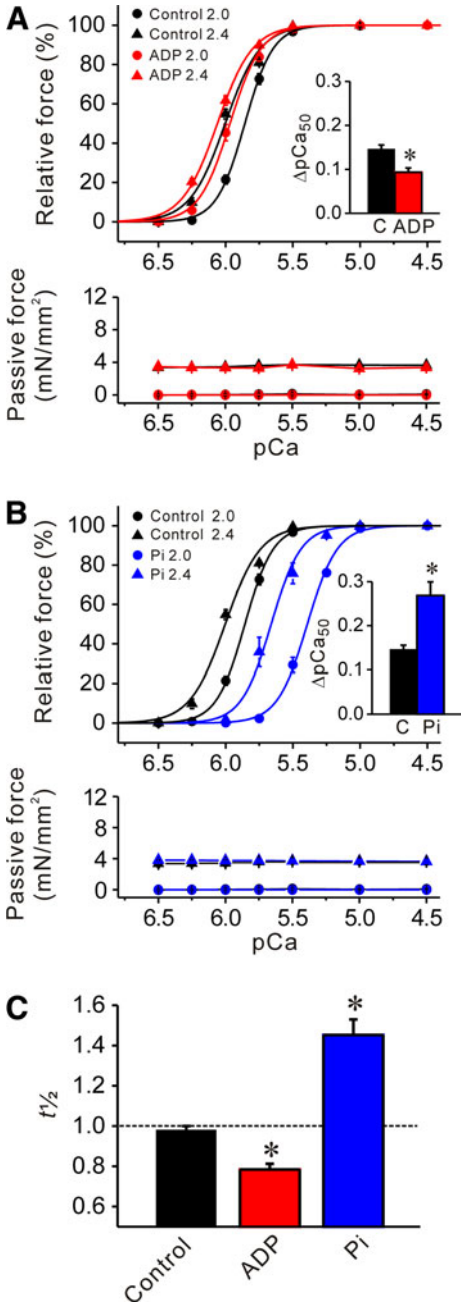

Fig. 2 Effects of MgADP or Pi on Ca^{2+} sensitivity and $t_{1/2}$ in rabbit psoas muscle fibers; SL 2.0 and 2.4 μm. **a** Effect of 3 mM MgADP on force–pCa curves (*top*) and passive force (*bottom*). *Black solid lines* −MgADP, *red solid lines* +MgADP. *Inset* comparison of ΔpCa_{50} in the absence and presence of MgADP. *C* control without MgADP. $^*P < 0.05$; $n = 6$. **b** Effect of 20 mM Pi on force–pCa curves (*top*) and passive force (*bottom*). *Black solid lines* −Pi (same as in **a**), *blue solid lines* +Pi. *Inset* comparison of ΔpCa_{50} in the absence and presence of Pi. $^*P < 0.05$; $n = 6$. Passive force was not significantly altered by MgADP or Pi at either 2.0 or 2.4 μm (**a**, **b**). **c** Comparison of $t_{1/2}$ in the absence and the presence of 3 mM MgADP or 20 mM Pi. $^*P < 0.05$ compared with control; $n = 6$

Table 1 Summary of the values of passive force, maximal active force, pCa_{50} and Hill coefficient (n_H) in rabbit psoas muscle fibers under various conditions (see Fig. 2)

	SL (μm)	Passive force (mN/mm^2)	Maximal force (mN/mm^2)	pCa_{50}	ΔpCa_{50}	n_H
Control	2.0	~0	168.50 ± 7.74	5.86 ± 0.01		4.12 ± 0.12
	2.4	3.58 ± 0.49	191.83 ± 8.98	6.00 ± 0.01	0.15 ± 0.01	3.31 ± 0.16
+ADP	2.0	~0	164.07 ± 20.64* (135.53 ± 18.46)	5.97 ± 0.02$^{\#}$		3.74 ± 0.12
	2.4	3.47 ± 0.20	184.79 ± 21.68	6.06 ± 0.01$^{\#}$	0.09 ± 0.01$^{\#}$	3.30 ± 0.16
+Pi	2.0	~0	85.14 ± 6.69$^{*,\#}$ (165.49 ± 15.15)	5.39 ± 0.01$^{\#}$		3.90 ± 0.26
	2.4	3.81 ± 0.27	144.23 ± 10.92$^{\#}$	5.66 ± 0.04$^{\#}$	0.27 ± 0.03$^{\#}$	3.93 ± 0.17$^{\#}$

Maximal force was obtained by activating muscle at pCa 4.5 prior to construction of the force–pCa curve at each SL (passive force was measured just prior to activation at pCa 4.5). Numbers in parentheses indicate maximal force values obtained prior to ADP or Pi application (* $P < 0.05$ compared with the prior value). Upon SL elongation from 2.0 to 2.4 μm, maximal force was significantly ($P < 0.05$) increased in all groups, due presumably to a change in the filament overlap (e.g., [5, 9])

$^{\#}$ $P < 0.05$ compared with the corresponding values in the control group (no ADP or Pi)

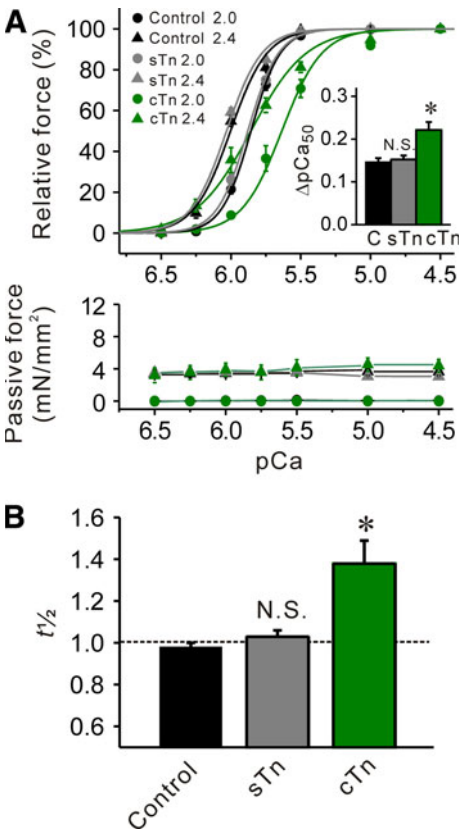

Fig. 3 Effects of sTn or cTn treatment on Ca^{2+} sensitivity and $t_{1/2}$ in rabbit psoas muscle fibers. **a** Effect of sTn or cTn treatment on force–pCa curves (*top*) and passive force (*bottom*). *Black solid lines* control without sTn or cTn treatment (same as in Fig. 2), *gray solid lines* sTn treatment, *green solid lines* cTn treatment. *Inset*, ΔpCa_{50} with and without Tn treatment. *C* control with no Tn treatment. *$P < 0.05$; $n = 5$ and 11 for sTn and cTn treatment, respectively. **b** Comparison of $t_{1/2}$ in the absence and the presence of sTn or cTn treatment. See [8] for the measurement of $t_{1/2}$ with Tn treatment. *$P < 0.05$ compared with control, *NS* not significant; $n = 5$ and 11 for sTn and cTn treatment, respectively

greater at SL 2.4 μm than at 2.8 μm, thereby increasing ΔpCa_{50} (Fig. 5c). The relative impact on SL-dependent Ca^{2+} activation by MgADP or Pi (~40 and ~75% for MgADP and Pi, respectively) was similar to that observed in experiments where SL was varied between 2.0 and 2.4 μm. The values of pCa_{50}, n_H and maximal force obtained in the absence or presence of MgADP or Pi are summarized in Table 3.

Figure 6 shows the relationship between passive force and the magnitude of SL-dependent Ca^{2+} activation in the absence and presence of MgADP or Pi, obtained in the short and long SL ranges. ΔpCa_{50} increased linearly as a function of passive force in the absence and the presence of MgADP or Pi ($P < 0.05$ in all cases), with the position of the regression line moved downward and upward, respectively, upon application of MgADP and Pi (slope was significantly increased by Pi but it was not significantly changed by MgADP).

Discussion

We demonstrated in the present study that the magnitude of SL-dependent Ca^{2+} activation in rabbit psoas muscle fibers depends on the level of thin filament cooperative activation in both short and long SL ranges (Figs. 2 and 5). Despite the same magnitude of elongation, SL-dependent Ca^{2+} activation was more pronounced in the long SL range, with the magnitude in linear proportion to passive force under varying degrees of thin filament cooperative activation (Fig. 6). We discuss these findings focusing on the role of thin filament cooperative activation in the regulation of SL-dependent Ca^{2+} activation in skeletal muscle.

As reported in our recent work on PLV [8], in the present study, MgADP accelerated the rate of rise of active

Table 2 Summary of the values of passive force, maximal active force, pCa_{50} and Hill coefficient (n_H) in rabbit psoas muscle fibers under various conditions (see Supplementary Fig. 1)

	SL (μm)	Passive force (mN/mm^2)	Maximal force (mN/mm^2)	pCa_{50}	ΔpCa_{50}	n_H
Control	2.0	~0	168.50 ± 7.74	5.86 ± 0.01		4.12 ± 0.12
	2.4	3.58 ± 0.49	191.83 ± 8.98	6.00 ± 0.01	0.15 ± 0.01	3.31 ± 0.16
+cTn	2.0	~0	145.24 ± 5.58*,# (173.66 ± 8.49)	5.64 ± 0.04#		3.02 ± 0.30#
	2.4	3.19 ± 0.91	186.12 ± 7.63	5.86 ± 0.04#	0.22 ± 0.02#	2.19 ± 0.10#
+sTn	2.0	~0	171.04 ± 6.44 (178.06 ± 7.59)	5.88 ± 0.01		3.94 ± 0.16
	2.4	3.78 ± 0.15	192.40 ± 7.50	6.03 ± 0.01	0.15 ± 0.01	3.41 ± 0.18

Values in the control group are the same as in those in Table 1. Maximal force was obtained by activating muscle at pCa 4.5 prior to construction of the force–pCa curve at each SL (passive force was measured just prior to activation at pCa 4.5). Numbers in parentheses indicate maximal force values obtained prior to cTn or sTn treatment (* $P < 0.05$ compared with the prior value). Upon SL elongation from 2.0 to 2.4 μm, maximal force was significantly ($P < 0.05$) increased in both cTn and sTn groups, due presumably to a change in the filament overlap (e.g., [5, 9])

# $P < 0.05$ compared with the corresponding values in the control group

force at low concentrations (1 and 3 mM), but MgADP decelerated it at a high concentration (10 mM) in rabbit psoas muscle fibers (Fig. 1). We consider that, at low MgADP concentrations, the actomyosin-ADP complex promotes cross-bridge attachment via enhanced thin filament cooperative activation (similar to the effect of *N*-ethylmaleimide-subfragment 1; e.g., [18, 19]), while at high MgADP concentrations, large fractions of the complex cause slowing of contraction operating as a dragging force (see [8] and references therein). On the other hand, Pi at low concentrations has been reported to decrease the fraction of the slowly cycling cross-bridges, resulting in acceleration of the rate of rise of active force (e.g., [8, 20]). However, as demonstrated previously by us in PLV, the application of high concentrations of Pi (e.g., 20 mM) is likely to decrease the fraction of strongly bound cross-bridges below a certain threshold value, resulting in slowing of contraction via reduced thin filament cooperative activation (Fig. 1). Therefore, under the present experimental settings, we consider that 3 mM MgADP enhances thin filament cooperative activation while 20 mM Pi reduces it in rabbit psoas muscle fibers. Here, one may point out that an alteration of thin filament cooperative activation is likely to change the n_H of the force–pCa curve, but no significant correlation existed between the n_H and ΔpCa_{50} in the present study (Supplementary Fig. 1; see also [8, 21] for cardiac muscle). However, it is still unknown whether or to what extent the n_H reflects thin filament cooperative activation (as discussed in detail in [8]). We therefore consider that, in skeletal muscle, as well as in cardiac muscle [8], $t_{1/2}$ more precisely reflects a sensitive change in thin filament cooperative activation than the n_H of the force–pCa curve.

It has been considered that a change in the overlap between the thick and thin filaments (or a change in the double-overlap between these filaments in the short SL

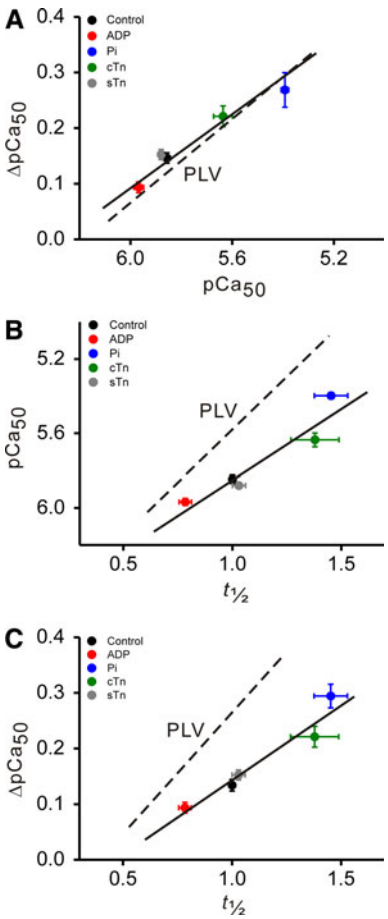

Fig. 4 Linear regression analyses between $t_{1/2}$, pCa_{50} and ΔpCa_{50}. **a** Relationship between pCa_{50} and ΔpCa_{50} ($R = 0.98$, $P < 0.0005$). **b** Relationship between $t_{1/2}$ and pCa_{50} ($R = 0.95$, $P < 0.05$). **c** Relationship between $t_{1/2}$ and ΔpCa_{50} ($R = 0.97$, $P < 0.01$). In (**a**–**c**), plots were constructed using the data in Figs. 2 and 3. pCa_{50} obtained at SL 2.0 μm. *Dashed lines* in (**a**–**c**) data obtained with PLV in our previous study [8] under the same experimental condition with SL varied between 1.9 and 2.3 μm. The values of pCa_{50} and $t_{1/2}$ were obtained at the slack SL (1.9 μm) for PLV

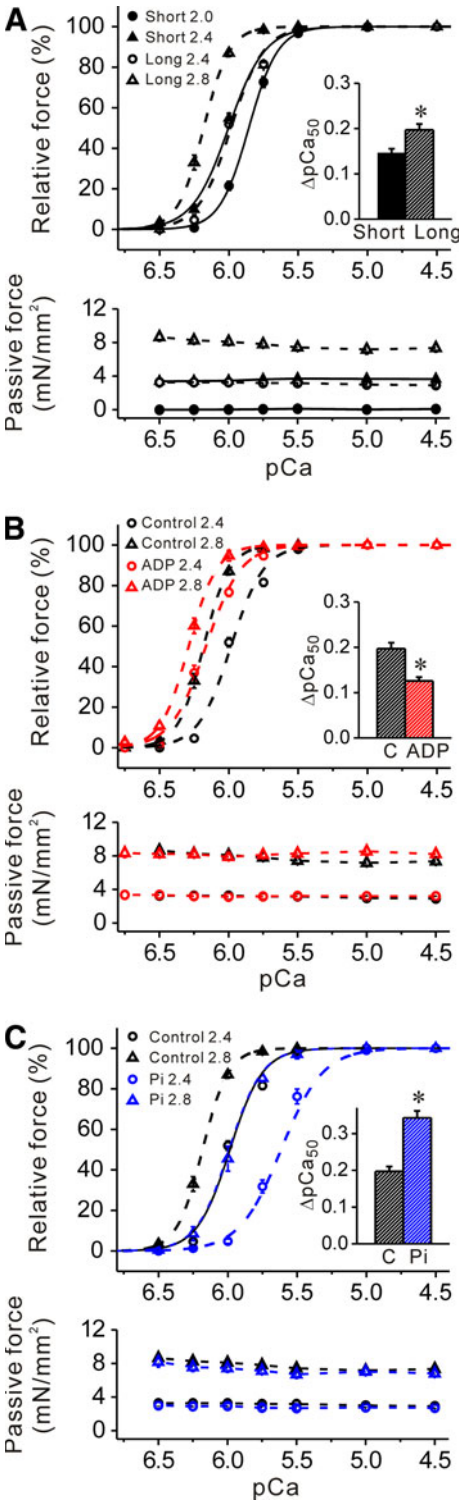

◀**Fig. 5** Effects of MgADP or Pi on Ca^{2+} sensitivity in rabbit psoas muscle fibers at SL 2.4 and 2.8 μm. **a** Comparison of force–pCa curves (*top*) and passive force (*bottom*) in the two different SL ranges [*short* (2.0 and 2.4 μm) and *long* (2.4 and 2.8 μm)] under the control condition without MgADP or Pi. Passive force was significantly ($P < 0.05$) greater at each point in the long SL range throughout the experiment [i.e., 2.0 μm (short) vs. 2.4 μm (long); 2.4 μm (short) vs. 2.8 μm (long)]. *Black solid lines* force–pCa curves in the short SL range (same as in Fig. 2). *Black dashed lines* force–pCa curves in the long SL range. *Inset* ΔpCa_{50} in the short and long SL ranges. $^*P < 0.05$; $n = 6$. **b** Effect of 3 mM MgADP on force–pCa curves (*top*) and passive force (*bottom*) in the long SL range. *Black dashed lines* (same as in **a**) –MgADP, *red dashed lines* +MgADP. *Inset* ΔpCa_{50} in the absence and presence of MgADP. *C* control without MgADP. $^*P < 0.05$; $n = 6$. **c** Effect of 20 mM Pi on force–pCa curves (*top*) and passive force (*bottom*) in the long SL range. *Black dashed lines* (same as in **a**, **b**) −Pi, *blue dashed lines* +Pi. *Inset* comparison of ΔpCa_{50} in the absence and presence of Pi. $^*P < 0.05$; $n = 6$. Passive force was not significantly altered by MgADP or Pi at either 2.4 or 2.8 μm (**b**, **c**)

range) underlies the basis for SL-dependent Ca^{2+} activation in skeletal muscle (e.g., [3]). We found in the present study that, in addition to the regulation via the filament overlap (as indicated by SL-dependent changes in maximal force; see Tables 1, 2 and 3), SL-dependent Ca^{2+} activation in skeletal muscle is influenced by thin filament cooperative activation (Fig. 4) and passive force (Fig. 6). Previously, by using PLV, we provided experimental as well as mathematical evidence that at high thin filament cooperative activation states, cross-bridge recruitment upon lattice spacing reduction due to titin extension becomes less pronounced due to a decrease in the fraction of "recruitable" cross-bridges (that have ATP and therefore can potentially produce active force), resulting in the attenuation of SL-dependent Ca^{2+} activation [8]. Therefore, the inverse correlation between the rate of rise of active force and ΔpCa_{50} (Fig. 4c) obtained by varying the level of thin filament cooperative activation, directly by Tn treatment or indirectly by application of MgADP or Pi, suggests that SL-dependent Ca^{2+} activation is regulated via "on–off" switching of the thin filament state in rabbit psoas muscle fibers, as in PLV [8].

The present findings (Figs. 2, 5) are consistent with the data obtained in PLV, suggesting that SL-dependent Ca^{2+} activation is modulated via thin filament cooperative activation in skeletal muscle, in coordination with titin-based lattice spacing modulation. The greater dependence of passive force in the presence of Pi (i.e., greater slope value in Fig. 6) is likely to suggest that cross-bridge recruitment via titin-based lattice spacing reduction is enhanced at low cooperative activation states, due to an increase in the fraction of "recruitable" cross-bridges (as demonstrated previously in cardiac muscle; see [8, 13]). Given the recent findings that the working SL range of skeletal muscle is relatively long in vivo (i.e., ~2.6 to ~3.0 μm in gastrocnemius muscle of mice, and ~3.0 to ~3.4 μm in extensor digitorum muscle of humans) [7], the greater SL-dependent Ca^{2+} activation in the longer SL range (Fig. 5; Table 3) may be a compensatory mechanism for the decrease in the filament overlap and subsequent reduction in active force. This possible compensatory effect may be of particular physiological significance under low force-

Table 3 Summary of the values of passive force, maximal active force, pCa_{50} and Hill coefficient (n_H) in rabbit psoas muscle fibers under various conditions (see Fig. 3)

	SL (μm)	Passive force (mN/mm^2)	Maximal force (mN/mm^2)	pCa_{50}	ΔpCa_{50}	n_H
Control	2.4	3.68 ± 0.36	189.33 ± 12.16	5.98 ± 0.01		3.67 ± 0.33
	2.8	8.65 ± 0.47	172.17 ± 9.82	6.18 ± 0.01	0.20 ± 0.01	4.64 ± 0.10
+ADP	2.4	3.68 ± 0.41	198.87 ± 7.68* (180.38 ± 9.45)	6.17 ± 0.02$^{\#}$		3.45 ± 0.09
	2.8	9.12 ± 0.63	183.87 ± 9.13	6.29 ± 0.02$^{\#}$	0.12 ± 0.01$^{\#}$	4.30 ± 0.14
+Pi	2.4	3.42 ± 0.30	133.17 ± 9.35$^{*,\#}$ (196.67 ± 4.59)	5.61 ± 0.02$^{\#}$		2.89 ± 0.26
	2.8	8.68 ± 0.69	118.50 ± 8.99$^{\#}$	5.99 ± 0.03$^{\#}$	0.34 ± 0.02$^{\#}$	3.65 ± 0.18$^{\#}$

Maximal force was obtained by activating muscle at pCa 4.5 prior to construction of the force–pCa curve at each SL (passive force was measured just prior to activation at pCa 4.5). Numbers in parentheses indicate maximal force values obtained prior to ADP or Pi application (*$P < 0.05$ compared with the prior value). Upon SL elongation from 2.4 to 2.8 μm, maximal force was significantly ($P < 0.05$) decreased in all groups, due presumably to a change in the filament overlap (e.g., [5, 9])

$^{\#}$ $P < 0.05$ compared with the corresponding values in the control group (no ADP or Pi)

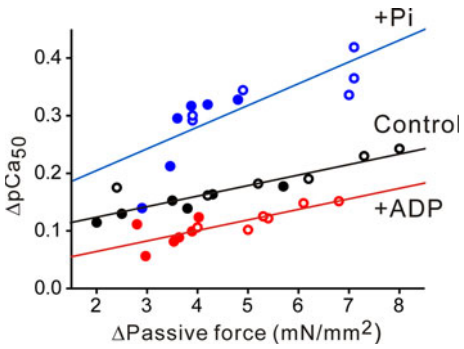

Fig. 6 Relationship between passive force and SL-dependent Ca^{2+} activation (ΔpCa_{50}) in the absence (*Control*) and presence of MgADP or Pi obtained in the short (2.0−2.4 μm: *closed symbols*) and long (2.4−2.8 μm: *open symbols*) SL ranges. Control, $Y = 0.0965 + 0.0166X$ ($R = 0.88$; $P < 0.0005$); MgADP, $Y = 0.0317 + 0.0175X$ ($R = 0.81$; $P < 0.005$); Pi, $Y = 0.132 + 0.0367X$ ($R = 0.78$; $P < 0.005$). The difference in slope was significant between the control and Pi groups (but not between the control and MgADP groups). ΔPassive force denotes the difference between the values of passive force at SL 2.0 and 2.4 μm (or at SL 2.4 and 2.8 μm)

generating states during fatigue (where the myoplasmic Pi concentration increases; see [11] and references therein), because the enhanced SL-dependent Ca^{2+} activation may have an effect to minimize the reduction in active force upon stretch at Ca^{2+} concentrations below the saturating level.

Konhilas et al. [22] demonstrated by using X-ray diffraction that an increase in SL from ∼2.0 to ∼4.0 μm linearly reduces the lattice spacing in both fast and slow skeletal muscles of the rat. More recently, Irving et al. [15] reported that passive force of several mN/mm^2 reduces the lattice spacing linearly with no significant effect on myosin mass transfer from the thick filament backbone to thin filaments in rabbit psoas muscle fibers, over the range of SL from 2.0 to 3.4 μm. In the present study, we found that the magnitude of SL-dependent Ca^{2+} activation was more pronounced in the long SL range than in the short SL range in the absence and the presence of MgADP or Pi (Figs. 2 and 5). We therefore consider that, in addition to the regulation via the filament overlap, titin-based passive force and subsequent lattice spacing reduction plays a pivotal role in regulating SL-dependent Ca^{2+} activation in skeletal muscle, with the magnitude depending on the state of the thin filaments (Fig. 6).

It was found that the slope of the linear regression line in the relationship of $t_{1/2}$ versus ΔpCa_{50} was ∼40% less in skeletal muscle than in cardiac muscle obtained under the same experimental condition (Fig. 4c; cf. [8]). This suggests that the dependence on thin filament cooperative activation in setting the magnitude of SL-dependent Ca^{2+} activation is ∼40% less in skeletal muscle than in cardiac muscle. Likewise, the lesser slope value for skeletal muscle in the relationship of $t_{1/2}$ versus pCa_{50} (∼30%; Fig. 4b) compared to that for cardiac muscle suggests that the positive feedback effect on Ca^{2+}-binding to TnC via cross-bridge formation due to enhanced thin filament cooperative activation is ∼30% less in skeletal muscle than in cardiac muscle. Therefore, these findings may in part account for the well-known phenomenon that SL-dependent Ca^{2+} activation is less in skeletal muscle than in cardiac muscle (cf. [6, 8, 10]).

In conclusion, our findings suggest that, in addition to the regulation via the filament overlap, SL-dependent Ca^{2+} activation in skeletal muscle is regulated via thin filament cooperative activation and titin-based lattice spacing modulation in a coordinated fashion. This is an area of future research to investigate whether and how the regulation is altered in sarcomeric disease, such as in various forms of skeletal muscle atrophy (e.g., [9, 11] and references therein).

Acknowledgments We thank Dr. Yuta Shimamoto (Rockfeller University, NY) for critical reading of our manuscript. We also thank Ms. Naoko Tomizawa (The Jikei University School of Medicine,

Tokyo, Japan) for technical assistance. The work of the authors was supported in part by Grants-in-Aid for Scientific Research from the Ministry of Education, Culture, Sports, Science and Technology of Japan (N.F. and S.K.) and by grants from the Japan Science and Technology Agency (CREST) (N.F.), the Vehicle Racing Commemorative Foundation (S.K.), the Institute of Seizon and Life Sciences (S.K.) and CASIO Science Promotion Foundation (N.F.).

References

1. Endo M (1972) Stretch-induced increase in activation of skinned muscle fibres by calcium. Nat New Biol 237:211–213
2. Allen DG, Kentish JC (1985) The cellular basis of the length-tension relation in cardiac muscle. J Mol Cell Cardiol 17:821–840
3. Gordon AM, Huxley, Julian FJ (1966) The variation in isometric tension with sarcomere length in vertebrate muscle fibres. J Physiol 184:170–192
4. Allen JD, Moss RL (1987) Factors influencing the ascending limb of the sarcomere length-tension relationship in rabbit skinned muscle fibres. J Physiol 390:119–136
5. Shimamoto Y, Kono F, Suzuki M, Ishiwata S (2007) Nonlinear force-length relationship in the ADP-induced contraction of skeletal myofibrils. Biophys J 93:4330–4041
6. Fukuda N, Terui T, Ohtsuki I, Ishiwata S, Kurihara S (2009) Titin and troponin: central players in the Frank–Starling mechanism of the heart. Curr Cardiol Rev 5:119–124
7. Llewellyn ME, Barretto RPJ, Delp SL, Schnitzer MJ (2008) Minimally invasive high-speed imaging of sarcomere contractile dynamics in mice and humans. Nature 454:784–788
8. Terui T, Shimamoto Y, Yamane M, Kobirumaki F, Ohtsuki I, Ishiwata S, Kurihara S, Fukuda N (2010) Regulatory mechanism of length-dependent activation in skinned porcine ventricular muscle: role of thin filament cooperative activation in the Frank–Starling relation. J Gen Physiol 136:469–482
9. Udaka J, Ohmori S, Terui T, Ohtsuki I, Ishiwata S, Kurihara S, Fukuda N (2008) Disuse-induced preferential loss of the giant protein titin depresses muscle performance via abnormal sarcomeric organization. J Gen Physiol 131:33–41
10. Terui T, Sodnomtseren M, Matsuba D, Udaka J, Ishiwata S, Ohtsuki I, Kurihara S, Fukuda N (2008) Troponin and titin coordinately regulate length-dependent activation in skinned porcine ventricular muscle. J Gen Physiol 131:275–283
11. Udaka J, Terui T, Ohtsuki I, Marumo K, Ishiwata S, Kurihara S, Fukuda N (2011) Depressed contractile performance and reduced fatigue resistance in single skinned fibers of soleus muscle after long-term disuse in rats. J Appl Physiol (Epub ahead of print)
12. Fukuda N, Kajiwara H, Ishiwata S, Kurihara S (2000) Effects of MgADP on length dependence of tension generation in skinned rat cardiac muscle. Circ Res 86:e1–e6
13. Fukuda N, O-Uchi J, Sasaki D, Kajiwara H, Ishiwata S, Kurihara S (2001) Acidosis or inorganic phosphate enhances length dependence of tension in rat skinned cardiac muscle. J Physiol 536:153–160
14. Fukuda N, Wu Y, Irving TC, Granzier H (2003) Titin isoform variance and length dependence of activation in skinned bovine cardiac muscle. J Physiol 553:147–154
15. Irving T, Wu Y, Bekyarova T, Farman GP, Fukuda N, Granzier H (2011) Thick-filament strain and interfilament spacing in passive muscle: effect of titin-based passive tension. Biophys J 100:1499–1508
16. Matsuba M, Terui T, O-Uchi J, Tanaka H, Ojima T, Ohtsuki I, Ishiwata S, Kurihara S, Fukuda N (2009) Protein kinase A-dependent modulation of Ca^{2+} sensitivity in cardiac and fast skeletal muscles after reconstitution with cardiac troponin. J Gen Physiol 133:571–581
17. Fukuda N, Sasaki D, Ishiwata S, Kurihara S (2001) Length dependence of tension generation in rat skinned cardiac muscle: role of titin in the Frank–Starling mechanism of the heart. Circulation 104:1639–1645
18. Swartz DR, Moss RL (1992) Influence of a strong-binding myosin analogue on calcium-sensitive mechanical properties of skinned skeletal muscle fibers. J Biol Chem 267:20497–20506
19. Swartz DR, Moss RL (2001) Strong binding of myosin increases shortening velocity of rabbit skinned skeletal muscle fibres at low levels of Ca^{2+}. J Physiol 533:357–365
20. Tesi C, Colomo F, Nencini S, Piroddi N, Poggesi C (2000) The effect of inorganic phosphate on force generation in single myofibrils from rabbit skeletal muscle. Biophys J 78:3081–3092
21. Dobesh DP, Konhilas JP, de Tombe PP (2002) Cooperative activation in cardiac muscle: impact of sarcomere length. Am J Physiol 282:H1055–H1062
22. Konhilas JP, Irving TC, de Tombe PP (2002) Length-dependent activation in three striated muscle types of the rat. J Physiol 544:225–236